

Geometrical description of the onset of multi-pulsing in mode-locked laser cavities

Feng Li,¹ P. K. A. Wai,¹ and J. Nathan Kutz^{2,*}

¹Photonics Research Centre, Department of Electronics and Information Engineering, The Hong Kong Polytechnic University, Hung Hom, Kowloon, Hong Kong SAR, China

²Department of Applied Mathematics, University of Washington, Seattle, Washington 98195-2420, USA

*Corresponding author: kutz@amath.washington.edu

Received May 11, 2010; revised August 10, 2010; accepted August 12, 2010;
posted August 12, 2010 (Doc. ID 128330); published September 23, 2010

A simple iterative model is introduced quantifying the interaction of saturable gain and nonlinear loss in a mode-locked laser cavity. The resulting geometrical description of the laser dynamics completely characterizes the generic multi-pulsing instability observed in experiments. The model further shows that the onset of multi-pulsing can be preceded by periodic and chaotic transitions as recently confirmed in theory and experiment. The results suggest ways to engineer the nonlinear losses in the cavity in order to achieve an enhanced performance. © 2010 Optical Society of America

OCIS codes: 140.4050, 140.3510, 140.3500, 060.3510.

1. INTRODUCTION

The onset of multi-pulsing as a function of increasing laser cavity energy is a well-known physical phenomenon [1,2] that has been observed in a myriad of theoretical and experimental mode-locking studies in both passive and active laser cavities [3–17]. Aside from two purely theoretical (computational) studies [3,4], the bulk of these observations has been almost exclusively experimental in nature. Specifically, each of these experiments demonstrates that as the gain pumping is increased, the number of mode-locked pulses in the cavity increases in an approximately linear and discrete manner with the cavity saturation energy. This observation is independent of the specific mode-locking mechanism used, whether it is nonlinear polarization rotation, nonlinear interferometry, quantum saturable absorbers, etc. Thus the phenomenon is ubiquitous to mode-locked laser cavities. One of the earliest theoretical descriptions of the multi-pulsing dynamics was by Namiki *et al.* [3], in which energy rate equations were derived for the averaged cavity dynamics. More recently, a full stability analysis of the mode-locking solutions was performed, showing that the transition dynamics between N and $N+1$ pulses in the cavity exhibited a more complex and subtle behavior than previously suggested [4]. Indeed, the theory predicted, and it has been confirmed experimentally since, that near the multi-pulsing transitions, both periodic and chaotic behavior could be observed as operating states of the laser cavity for a narrow range of parameter space [4–7]. In this paper, we generalize the energy rate equation approach [3] and develop an iterative technique that provides a simple geometrical description of the entire multi-pulsing transition behavior as a function of increasing cavity energy. The model captures all the key features observed in experiment, including the periodic and chaotic mode-locking regions [5], and it further provides valuable insight into

laser cavity engineering for maximizing the performance, i.e., enhancing the mode-locked pulse energy.

The multi-pulsing instability arises from the competition between the laser cavities' bandwidth constraints and the energy quantization associated with the resulting mode-locked pulses, i.e., the so-called soliton area theorem [3]. Specifically, as the cavity energy is increased, the resulting mode-locked pulse has increasing peak power and spectral bandwidth. The increase in the mode-locked spectral bandwidth, however, reaches its limit once it is commensurate with the gain bandwidth of the cavity. Further increasing the cavity energy pushes the mode-locked pulse to an energetically unfavorable situation where the pulse spectrum exceeds the gain bandwidth, thereby incurring a spectral attenuation penalty. In contrast, by bifurcating to a two-pulse per round trip configuration, the pulse energy is then divided equally between two pulses whose spectral bandwidths are well contained within the gain bandwidth window. Figure 1 illustrates the concept as a function of increasing gain.

To theoretically characterize the multi-pulsing transition, a model is needed that is capable of capturing the dynamic competition between the various multi-pulse solution branches. Often it is the case that various of these branches are stable at the same time, thus leading to bistable behavior in the system [3–17]. Starting from initial white noise in the laser cavity, an effective model must select which branch of solutions is selected in the mode-locking process. In the model constructed here, a minimal set of assumptions are made. First, the cavity is assumed to have a nonlinear loss due to the cavities' saturable absorption. Second, the cavity is subject to bandwidth limited saturable gain. Third, upon undergoing a multi-pulsing bifurcation, the resulting pulses are well-separated in time. With these three assumptions, a geometrical iteration picture can be constructed of the

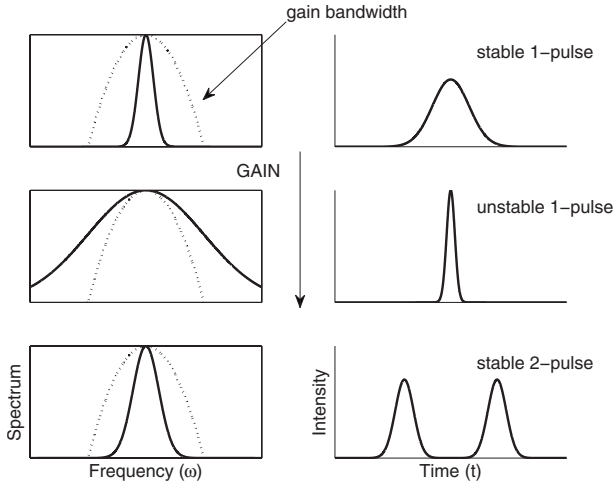


Fig. 1. Multi-pulsing bifurcation dynamics as a function of increasing gain. As the gain is increased, the mode-locked pulse peak power and spectral width (bold lines) are increased beyond the gain bandwidth (dashed line), leading to the formation of two mode-locked pulses whose spectra are within the gain bandwidth.

multi-pulsing dynamics by considering the intersection of the gain and loss curves that are applied once per round trip. It is a simple model that yields tremendous insight into the more subtle and complex issues of the multi-pulsing dynamics observed theoretically and experimentally [4,5,7]. Further, it is a much simpler analytical framework to understand than previous theoretical findings [3,4].

The paper is outlined as follows: In Section 2, the principle of operation is outlined for the multi-pulsing analysis. This is the key section of the paper, highlighting the geometrical viewpoint of the multi-pulsing bifurcation analysis. Section 3 considers explicit numerical simulations of the geometrical model for the three key saturation curves of physical interest. This gives a quantitative measure of the multi-pulsing instability. Section 4 discusses a method by which the nonlinear losses can be engineered to achieve key mode-locking characteristics such as high-energy pulses or self-starting. A review of the findings and concluding remarks are found in Section 5.

2. PRINCIPLE OF OPERATION

The aim of this section is to provide a high-level overview of the formal theoretical framework needed to capture the multi-pulsing mode-locking dynamics. The discussion will evolve around a geometrical representation of the dynamics, and three key papers are of critical importance [3–5]. The simplified theoretical framework considered here involves a balance between two dominant physical effects: the nonlinear loss and the saturating gain. Figure 2 illustrates the simplified cavity that is driven by the saturating gain and nonlinear losses. The remaining physical effects, discussed in what follows, are balanced in the formation of the mode-locked pulse [3].

The primary modeling component in the paper by Namiki *et al.* [3] is the development of an energy rate equation. In this formulation, the mode-locked pulse energy is computed over one round trip. The exact form of

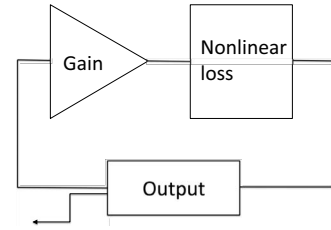


Fig. 2. Simple cavity configuration involving a saturable gain element and a nonlinear loss element that gives the cavity saturable absorption. The remaining physical effects are assumed to balance each other in the formation of a mode-locked pulse.

the mode-locked pulse solution is unimportant, and it is assumed that the effects of chromatic dispersion, self-phase modulation, nonlinear gain, and the bandwidth gain limitations effectively balance each other to form the mode-locked pulse solution [3]. Indeed, the fundamental premise of mode-locking is that a localized pulse solution exists for a given balance of dispersive and dissipative effects [1,2]. For more on such dissipative solitons, see Akhmediev and Ankiewicz [18]. Unlike the work of Namiki *et al.* [3], the model formulation established here treats the cavity as a discrete loss-gain system so that the cavity dynamics are understood from an underlying iteration scheme.

Before proceeding to the analysis, a few comments are made about the variable naming conventions used in the paper and their relation to Fig. 2. The variable E will represent the cavity energy. However, it will rarely appear without superscripts or subscripts when referring to the laser cavity. The subscript *in* or *out* will refer to the energy at the input or output of a laser cavity element, respectively. The superscripts *loss* and *gain* will refer to the laser cavity element under consideration. For instance, the expression E_{out}^{gain} refers to the output energy of the gain element. Additionally, the expression E_j refers to the energy of the j th pulse at the output coupler (see Fig. 2), and E_{total} is the sum of energies of all the pulses. The final term, E_{sat} , is the saturation energy of the gain medium which is modified in practice as the gain pumping is adjusted in the laser cavity.

A. Saturating Gain

We will make the same assumptions as those laid out by Namiki *et al.* [3] and will simply consider a model for the saturating gain as well as the nonlinear cavity losses. Figure 2 shows the basic laser cavity configuration considered. The two primary components of loss and gain are included. The saturating gain dynamics results in the following differential equation for the gain [1–3]:

$$\frac{dE_j}{dZ} = \frac{g_0}{1 + \sum_{j=1}^N E_j/E_{sat}} E_j, \quad (1)$$

where E_j is the energy of the j th pulse ($j=1, 2, \dots, N$), g_0 measures the gain pumping strength, and E_{sat} is the saturation energy of the cavity. The total gain in the cavity can be controlled by adjusting the parameter g_0 or E_{sat} . In what follows here, the cavity energy will be increased by simply increasing the cavity saturation parameter E_{sat} . This increase in the cavity gain can equivalently be controlled by adjusting g_0 . These are generic physical param-

eters that are common to all laser cavities, but which can vary significantly from one cavity design to another. The parameter N is the number of pulses in the cavity [4]. This parameter, which is critical in the following analysis, helps to capture the saturation energy received by each individual pulse. Note that this equation can be solved exactly using standard methods of differential equations. However, the resulting solution is given in an implicit form.

B. Nonlinear Loss (Saturable Absorption)

The nonlinear loss in the cavity, i.e., the saturable absorption or saturation fluency curve, will be modeled by a simple transmission function:

$$E_{out} = T(E_{in})E_{in}. \quad (2)$$

The actual form of the transmission function $T(E_{in})$ can vary significantly from experiment to experiment, especially for very high input energies. For instance, for mode-locking using nonlinear polarization rotation, the resulting transmission curve is known to generate a periodic structure at higher intensities. Alternatively, an idealized saturation fluency curve can be modified at high energies due to higher-order physical effects. As an example, in mode-locked cavities using waveguide arrays [4], the saturation fluency curve can turn over at high energies due to the effects of three-photon absorption, for instance. As a final note, this transmittance function is commonly referred to in the literature as the cavity's nonlinear loss or saturable absorption [1–3]. In what follows, the terms *nonlinear loss* and *transmission curves* will be used interchangeably.

A number of specific nonlinear loss curves will be considered in the next section. For the moment, however, consider the rather generic saturation curve as displayed in Fig. 3. This shows the output energy as a function of the input energy. It is assumed, for illustrative purposes, that some higher-order nonlinear effects cause the saturation curve to turn over at high energies. This curve describes the nonlinear losses in the cavity as a function of increasing input energy for N mode-locked pulses. Also plotted in Fig. 3 is an analytically calculated line that gives a threshold value for multi-pulsing operation. The

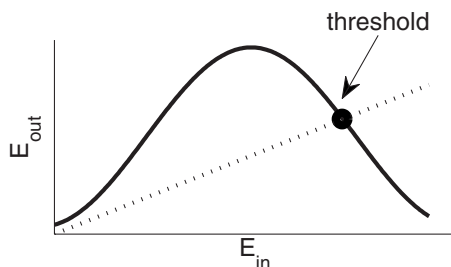


Fig. 3. Generic nonlinear loss (or saturable absorption or saturable fluency) curve (bold line) showing the standard effect of saturable absorption at high energies along with a fold-over due to higher-order nonlinear loss processes. The dashed line is the analytically computed threshold curve. Once the input energy is increased above the threshold point, any perturbation will cause the growth of an additional pulse, so the cavity jumps from N to $N+1$ pulses. Note that the small and large signal transmission curves (dashed and solid lines, respectively) coalesce for low input energies.

threshold is the small signal loss (constant loss of the cavity) that limits the amplification of small signals. In laser cavities, any signal with a gain larger than the loss is amplified. For small signals, only the linear part of the nonlinear loss will take effect, and if the gain in the cavity is larger than this constant loss, the small signals will be amplified. When there is already a large pulse in the cavity, due to gain saturation, the gain value can be smaller than the constant loss. Because the pulses in same round trip are assumed to see the same gain, i.e., the slow saturation assumption, then any perturbation (small pulses) will be suppressed, because the gain is less than the loss for them. With the increase of the parameter E_{sat} , the gain for the larger pulses increases. Since it is larger than the constant loss, the perturbations (small pulses) in the cavity will be amplified to large pulses, and more pulses will be generated. As more pulses join the multi-pulsing configuration, the entire gain in the cavity will be saturated again and drop to lower than the constant loss. This new stable configuration will remain stable until the saturated energy E_{sat} is further increased.

C. Iterative Cavity Dynamics

The generic loss curve illustrated in Fig. 3 along with the saturable gain as a function of the number of pulses [Eq. (1)] are the only two elements required to completely characterize the multi-pulsing transition dynamics and bifurcation. When considering the cavity configuration in Fig. 2, the alternating action of saturating gain and nonlinear loss produces an iteration map which only has pulses whose loss and gain balance is stabilized in the cavity. Specifically, the output of the gain is the input of the nonlinear loss, and vice versa. This is much like the logistic equation iterative mapping for which a rich set of dynamics can be observed with a simple nonlinearity [19,20]. Indeed, the behavior of the multi-pulsing system is qualitatively similar to the logistic map with steady-state, periodic, and chaotic behavior all potentially observed in practice.

In addition to the connection with the logistic equation framework, two additional features are particular to our problem formulation. First, we have multiple branches of stable solutions, i.e., the one-pulse, two-pulse, three-pulse, etc. Second, the loss curve exceeds the threshold energy as shown in Fig. 3. Figure 4 is the key figure of the paper and exhibits all the critical features of our multi-pulsing model. Exhibited in this model are the input and output relationships for the gain and loss elements of Fig. 2. Three gain curves are illustrated for Eq. (1) with $N=1$, $N=2$, and $N=3$. These correspond to the one-pulse, two-pulse, and three-pulse per round trip solutions, respectively. The intersection of the loss curve with a gain curve represents the mode-locked solutions. These two curves are the ones on which the iteration procedure occurs [19,20]. As the gain is increased through the cavity saturation energy E_{sat} , the gain solution curves move to the right in the graph, producing steady-state (a), periodic (b) and chaotic (c) behavior (see Fig. 5 for how the iteration generates these types of behavior). Such differing types of behavior are common to nonlinear iteration maps [19,20]. In the current scenario, the one-pulse solution branch has reached a point in the solution space where the iteration

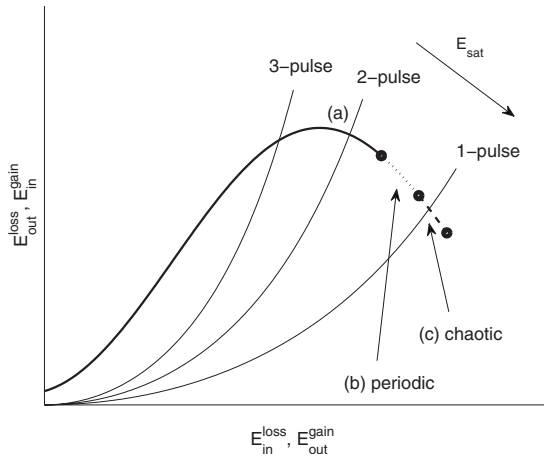


Fig. 4. Nonlinear loss and saturating gain curves for one-pulse ($N=1$), two-pulse ($N=2$), and three-pulse ($N=3$) per round trip configurations. The intersection of the gain and loss curves represents the mode-locked solution states of interest. As the gain parameter g_0 is increased, the gain curves shift to the right. The one-pulse solution first becomes periodic (b), and then chaotic (c) before ceasing to exist since it no longer intersects the loss curve. The solution then jumps to the next most energetically favorable configuration of two pulses per round trip (a). This qualitative picture describes the entire N to $N+1$ pulse transition.

between the gain and loss dynamics produces chaotic energy fluctuations in the laser cavity. If the gain is further increased, the one-pulse solution branch moves past the threshold point, and no one-pulse per round trip solutions are stable any longer. Instead, the mode-locking moves to a multi-pulsing configuration with a higher number of pulses.

Generically, this process of increasing the gain shows explicitly how the mode-locked laser jumps from N to $N+1$ pulses per round trip. It is simply a consequence of the N solution branch exceeding the threshold point of the nonlinear loss curve where that particular solution no longer is stable. This forces the dynamics to a higher number of pulses per round trip. Moreover, depending on the curvature of the nonlinear loss curve for high-energy, the transition dynamics can exhibit periodic (b) and chaotic dynamics (c) before the onset of steady-state multi-pulsing (a).

Figure 5 demonstrates the iterative process for the generic gain and loss curves illustrated in Fig. 4. Specifically, the production of steady-state [Fig. 5(a)], periodic [Fig. 5(b)], and chaotic [Fig. 5(c)] behavior in the system is illustrated. These curves are standard iteration curves produced when considering, for instance, the logistic equation [19,20].

As stated previously in the paper, the onset of multi-pulsing behavior through periodic and chaotic regions has been verified through both experiment [5] and direct numerical simulations of a full laser cavity model based on waveguide arrays [4]. To explicitly make connection to the laser cavity pulse dynamics, Fig. 6 illustrates the behavior in the laser cavity as a function of increasing cavity saturation energy E_{sat} . As E_{sat} is increased through four successively higher values, the stable one-pulse solution [corresponding to (a) in Fig. 5] first undergoes a Hopf bifurcation to a periodic breather [corresponding to (b) in Fig. 5] before becoming chaotic [corresponding to (c) in

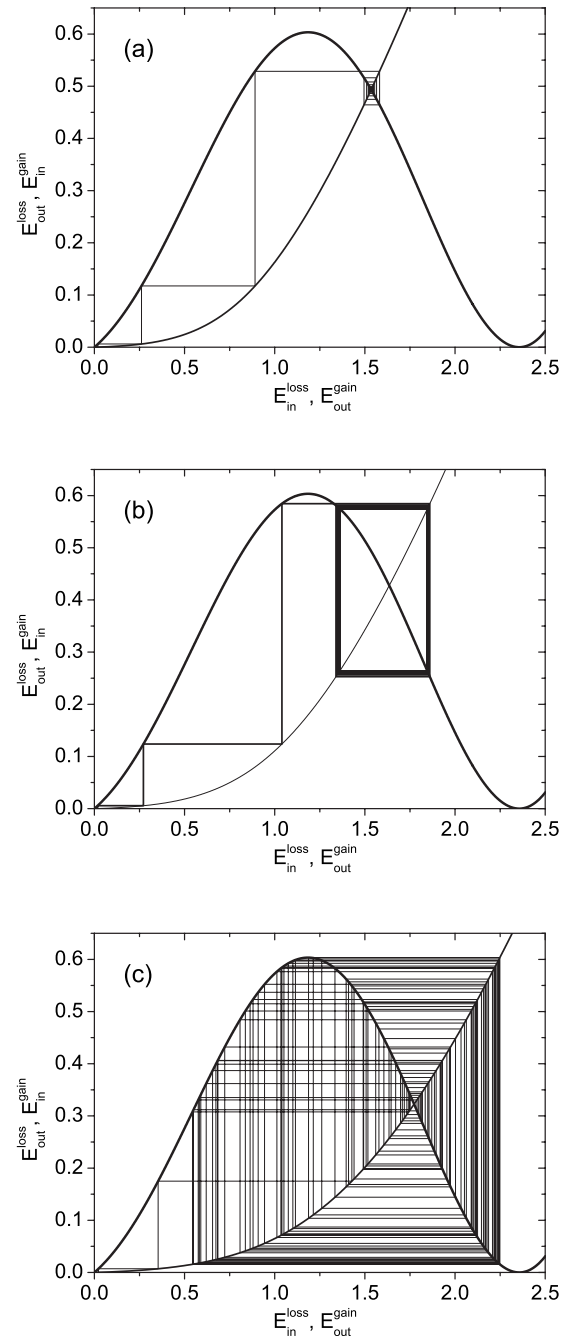


Fig. 5. Iteration map dynamics for the nonlinear loss and saturating gain behavior. Possible iteration behaviors are (a) a steady-state solution, (b) a periodic solution, and (c) a chaotic dynamics. The interpretation of the periodic and chaotic dynamics in the mode-locking is given in Fig. 6. Note that the periodic and chaotic dynamics arise before the onset of multi-pulsing for the nonlinear loss curve chosen here.

Fig. 5] and finally achieving the stable two-pulse solution [corresponding once again to (a) for the two-pulse branch in Fig. 5]. Details of the parameters and model used for this simulation are found in [4].

This concludes our section on the principle of operation. Once the graph in Fig. 4 is understood, the transition that processes from N to $N+1$ can be understood along with the potential periodic and chaotic dynamics preceding the transition. In what follows, various explicit forms of the

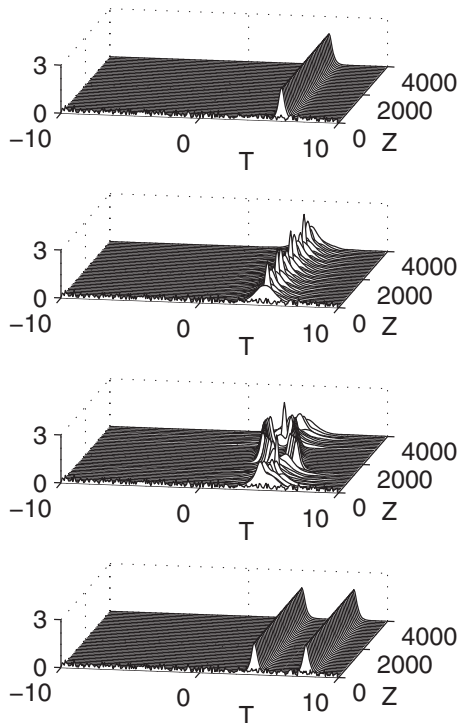


Fig. 6. Mode-locked cavity simulation where the saturable absorption is provided by waveguide arrays [4]. Shown is the intensity of the mode-locked field as a function of normalized propagation distance Z and time T . As the cavity gain is increased via g_0 , the stable one-pulse configuration first bifurcates to a periodic solution, and then bifurcates again to a chaotic solution, before finally going to the two-pulse configuration.

loss curve will be considered. By appropriate engineering of the nonlinear loss curve, the periodic and chaotic transition effects can be mitigated.

3. MULTI-PULSING TRANSITION DYNAMICS

Until now, the figures presented demonstrate the qualitative picture of the underlying dynamics associated with the onset of multi-pulsing. In this section, several specific transmission (nonlinear loss) curves will be constructed, and their dynamics will be investigated. The key observation is that engineering of the nonlinear loss curve can have significant impact on the laser cavity dynamics. Thus although the nonlinear loss curves do not necessarily correspond to any real laser cavity, one can imagine that by engineering a laser cavity, one can potentially observe all of the dynamics demonstrated in what follows.

To be more explicit about the simulations presented, the iteration algorithm used in what follows is outlined. Thus the simulation results are carried out as follows:

(i) The cavity saturation parameter E_{sat} is scanned starting from an initial value of $E_{sat}=0.001 \ll 1$. It is assumed that initially there are a total of $N=10$ pulses of small amplitude ($E_j \sim O(10^{-8})$) in the cavity. Note that the resulting pulse separation dynamics is not considered in the analysis [3].

(ii) Input the initial signal field into the governing saturable gain equation (1). Solve this equation with a

standard time-integration method, such as fourth-order Runge–Kutta, or solve for E_j from the exact implicit solution representation.

(iii) Input the signal from the gain element into the nonlinear loss element [Eq. (2)]. Mathematically, this action is represented by its transmission function.

(iv) Iterate Steps (ii) and (iii) until the output converges. If the solution fails to converge to a fixed point, i.e., when the iteration produces periodic or chaotic dynamics, use the last 256 iterations as a representation of the dynamics. The last iteration of the E_j values is used as the seed for the next value of increasing E_{sat} .

(v) Increase E_{sat} by $\Delta E_{sat}=0.001$. Add small perturbations to the E_j values obtained from the previous E_{sat} iteration in step (iv). These are the new initial values for E_j in Eq. (1).

(vi) Repeat Steps (iv) and (v).

With $N=10$, this simple algorithm allows us to fully explore the transition dynamics until ten pulses are generated in the cavity. Note that N is chosen arbitrarily and could be made much larger than 10. However, in the results presented here, we do not consider any simulations where more than ten pulses are generated per round trip.

A. Example 1: Transition without Chaos

To begin, an example of a transmission curve will be considered that mitigates any periodic or chaotic mode-locking in the cavity. For this case, Eq. (1) is considered with $N=10$ and for a propagation distance of $Z=1$. For convenience, the gain pumping strength is held fixed at $g_0=\log(100)$. To adjust the effective cavity energy, the saturation energy E_{sat} of the cavity is modified. Recall that the overall gain can be modified through either g_0 or E_{sat} . The specific form of the transmission considered is given by

$$T(E) = 0.5e^{-\alpha_1(E - \alpha_2)^8} + 0.1e^{-\alpha_1(E - \alpha_2)^2}, \quad (3)$$

with $\alpha_1=0.5$ and $\alpha_2=0.8$.

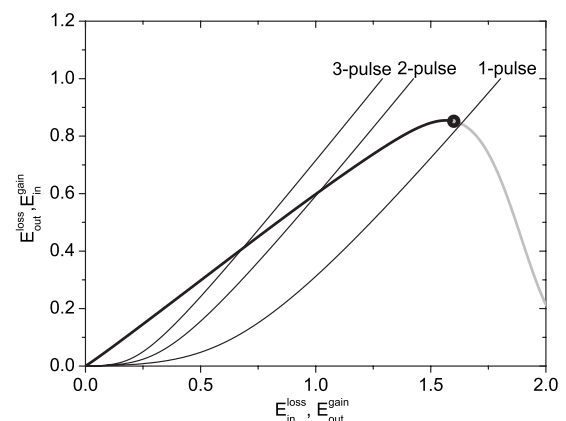


Fig. 7. Nonlinear loss and saturating gain curves for one-pulse, two-pulse, and three-pulse per round trip configurations. The intersection of the gain and loss curves represents the mode-locked solution states of interest. As the cavity energy is increased, the gain curves shift to the right. For this case, the one-pulse solution ceases to exist beyond the threshold point indicated by the bold circle. Thus no periodic or chaotic behavior arises. The solution then jumps to the most energetically favorable configuration of two pulses per round trip.

Figure 7 gives the quantitative versions of the curves qualitatively represented in Fig. 4. Specifically, the nonlinear loss curve along with the gain curves of the one-pulse, two-pulse, and three-pulse mode-locked solutions are given along with the threshold point. As the cavity energy is increased through an increasing value of E_{sat} , the one-pulse solution becomes unstable to the two-pulse solution as expected. In this case, the computed threshold value does not extend down the loss curve to where the periodic and chaotic branches of solutions occur; thus no periodic and chaotic dynamics are observed. Rather, a clean multi-pulsing bifurcation occurs as depicted in Fig. 8. In this case, the total cavity energy along with the single pulse's energy is depicted as a function of increasing gain. This curve is in complete agreement with numerous experimental and theoretical findings [3–17]. Specifically, each of these experiments demonstrates that as the gain pumping is increased, the number of pulses in the cavity increases in an approximately linear and discrete manner as demonstrated in Fig. 8.

B. Example 2: Transition with Chaos

A more interesting and subtle behavior can occur in the multi-pulse bifurcation structure with only a slight change to the transmission function in Eq. (2). Consider changing a single parameter by 25% so that the parameter $\alpha_2=1$ in Eq. (2). This slight change completely changes the nature of the bifurcation structure observed in Figs. 7 and 8.

Figure 9 now gives the quantitative versions of the curves qualitatively presented in Fig. 4. Specifically, the nonlinear loss curve along with the gain curves of the one-pulse, two-pulse, and three-pulse mode-locked solutions are given along with the threshold point as before. As the cavity energy is increased through an increasing value of E_{sat} , the one-pulse solution becomes unstable to the two-pulse solution as expected. In this case, the computed threshold value does extend down the loss curve to where the periodic and chaotic branches of solutions occur, thus allowing for the observation of periodic and chaotic dynamics. The multi-pulsing bifurcation occurs as depicted in Fig. 10. The total cavity energy along with the single

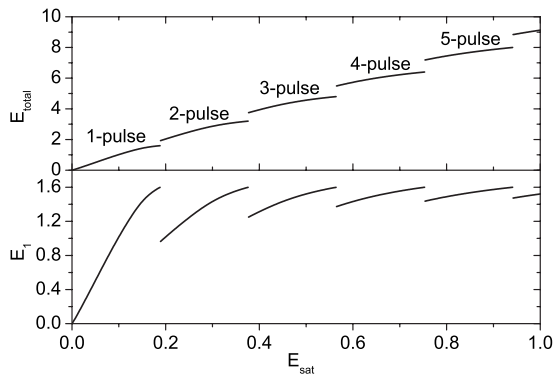


Fig. 8. Iteration map dynamics for the nonlinear loss and saturating gain behavior of Fig. 7. Shown is the total cavity energy E_{out} (top panel) and the individual pulse energy E_1 (bottom panel) as functions of the cavity saturation energy E_{sat} . The transition dynamics between multi-pulse operations produces a discrete jump in the cavity energy. In this case, no periodic or chaotic dynamics is observed.

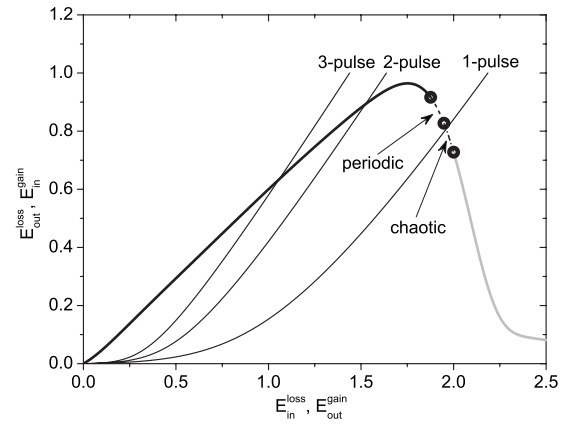


Fig. 9. Nonlinear loss and saturating gain curves for one-pulse, two-pulse, and three-pulse per round trip configurations. The intersection of the gain and loss curves represents the mode-locked solution states of interest. As the cavity energy is increased, the gain curves shift to the right. Unlike Fig. 7, the one-pulse solution first experiences periodic and chaotic behavior before ceasing to exist beyond the threshold point indicated by the right-most bold circle. The solution then jumps to the next most energetically favorable configuration of two pulses per round trip.

pulse's energy is depicted as a function of increasing gain. For this case, which is only a slight modification of the previous dynamics, the solution first undergoes a Hopf bifurcation to a periodic solution. Through a process of period doubling reminiscent of the logistic map [19,20], the solution goes chaotic before eventually transitioning to the two-pulse per solution branch. This process repeats itself with the transition from N to $N+1$ pulses generating periodic and then chaotic behavior before the transition is complete. This curve is in complete agreement with recent experimental and theoretical findings [4–6], thus validating the predicted dynamics.

One of the more interesting consequences of the transition with chaos is the randomness that is introduced in the multi-pulsing bifurcation. In particular, the chaotic behavior does not guarantee a transition from N to $N+1$

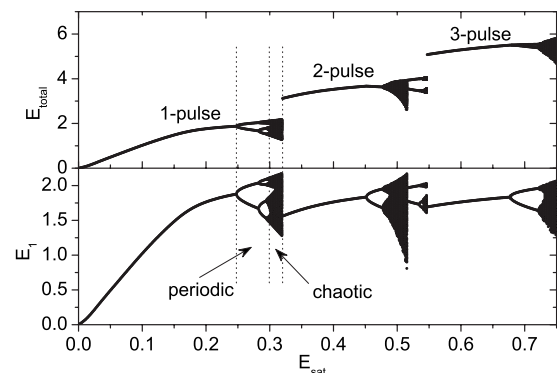


Fig. 10. Iteration map dynamics for the nonlinear loss and saturating gain behavior of Fig. 9. Shown is the total cavity energy E_{out} (top panel) and the individual pulse energy E_1 (bottom panel) as functions of the cavity saturation energy E_{sat} . The transition dynamics between multi-pulse operations produces a discrete jump in the cavity energy. In this case, both periodic and chaotic dynamics are observed preceding the multi-pulsing transition. This is consistent with recent theoretical and experimental findings [4–6].

pulses. Rather, a transition from N to $N+m$ pulses occurs. As different realizations of this numerical experiment are run, the N to $N+m$ random transition is easily observed, especially for a higher number of pulses in the cavity. Figure 11 demonstrates two simulations for increasing saturation energy. Note that in both cases, for a higher number of pulses in the cavity, the transition is not from N to $N+1$ pulses, but rather from N to $N+m$ pulses. It should be noted that this behavior is in contrast to laser cavities that do not have a chaotic transition region. Indeed, in such laser cavities where transition occurs without chaos, the transition is always from N to $N+1$ pulses.

C. Example 3: Periodic Nonlinear Loss

Finally, a periodic transmission profile is considered. This transmission profile is inspired by laser cavities mode-locked through the process of nonlinear polarization rotation. In such cases, the transmission curve is known to be periodic in nature. To model the transmission profile, we consider the transmission function of the form

$$T(E) = 0.1 + 0.2[1 + \cos(2E - 0.8\pi)], \quad (4)$$

where $T(E)$ now has a periodic component as might be expected in a nonlinear polarization rotation based laser.

Figure 12 gives the quantitative versions of the curves qualitatively presented in Fig. 4, but now extended for large values of energy due to the periodic nature of the transmission. Specifically, the nonlinear loss curve along with the gain curves of the one-pulse, two-pulse, and

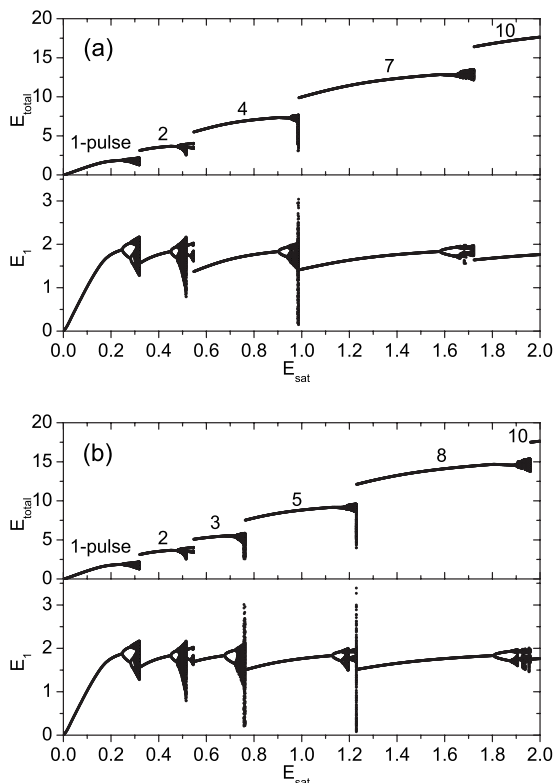


Fig. 11. Iteration map dynamics for the periodic nonlinear loss and saturating gain behavior of Fig. 9. Shown is the total cavity energy E_{out} (top panel) and the individual pulse energy E_1 (bottom panel) as functions of the cavity saturation energy E_{sat} for two simulations. The transition dynamics shows that the chaotic behavior generates a more generic N to $N+m$ pulses bifurcation.

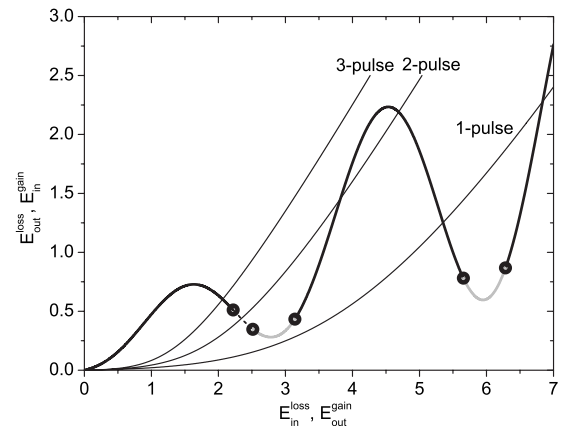


Fig. 12. Periodic nonlinear loss and saturating gain curves for one-pulse, two-pulse, and three-pulse per round trip configurations. The intersection of the gain and loss curves represents the mode-locked solution states of interest. As the cavity energy is increased, the gain curves shift to the right. The one-pulse solution first experiences periodic and chaotic behavior before ceasing to exist beyond the threshold point indicated by the rightmost bold circle. The solution then jumps to the next most energetically favorable configuration of two pulses per round trip. However, a high-energy one-pulse solution can also exist.

three-pulse mode-locked solutions are given along with the threshold points. The periodic nature of the solution suggests that higher-energy solutions may be accessible in the mode-locking process. As the cavity energy is increased through an increasing value of E_{sat} , the one-pulse solution becomes unstable to the two-pulse solution as expected. In this case, the computed threshold value only extends down the loss curve to where the periodic branch of solutions occurs; thus no chaotic dynamics are observed in the first transition to a periodic or chaotic two-pulse solution. As previously, the total cavity energy along with the single pulse’s energy is depicted as a function of increasing gain in Fig. 13.

4. ENGINEERING CAVITY LOSSES

The three examples given in the preceding section highlight the three transition behaviors that can occur: (i)

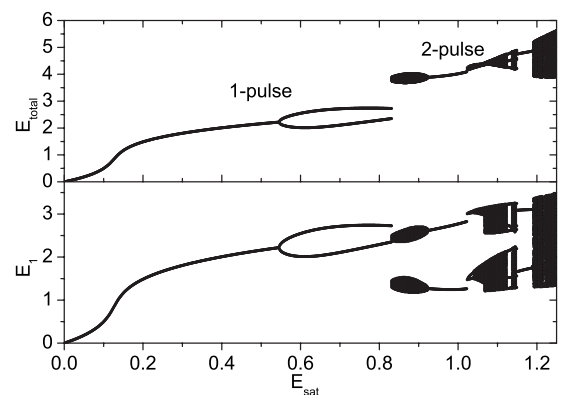


Fig. 13. Iteration map dynamics for the periodic nonlinear loss and saturating gain behavior of Fig. 12. Shown is the total cavity energy E_{out} (top panel) and the individual pulse energy E_1 (bottom panel) as functions of the cavity saturation energy E_{sat} . The transition dynamics between multi-pulse operations produces a discrete jump in the cavity energy. In this case, periodic dynamics is observed preceding the multi-pulsing transition to chaotic two-pulse solutions.

multi-pulsing transition without periodic or chaotic behavior, (ii) multi-pulsing transition with periodic but not chaotic behavior, and (iii) multi-pulsing transition with both periodic and chaotic transitions. Only small changes to the nonlinear loss curve can generate all three scenarios.

The sensitivity to all three scenarios suggests that engineering of the nonlinear gain in the cavity, i.e., the transmission curve [Eq. (2)], can potentially lead to gains in the performance or larger operating regimes. But what is of greatest interest is an observation associated with example 3 considered above. It is interesting to note that a higher-energy solution now exists for the one-pulse per round trip configuration due to the periodic nature of the transmission curve. Thus it is possible to jump to this solution rather than the two-pulse per round trip scenario. However, the interplay of total cavity energy and the nonlinear loss typically forces the cavity to select the most energetically favorable operating regime. This would be the two-pulse per round trip scenario versus the high-energy one-pulse per round trip scenario. However, the high-energy branch of solutions is accessible provided the laser cavity initial conditions are prepared carefully. This is typically not done since the laser cavity is self-starting from white noise.

However, one can always ask the following question: is it possible to engineer the cavity such that the higher-energy solution branch is favored over multi-pulsing? We show that indeed this can be done. Two examples are given of nonlinear loss curves that generate the high-energy one-pulse solutions as functions of increasing cavity energy. In the first example, illustrated in Figs. 14 and 15, a discrete jump is observed in the cavity energy much like the multi-pulsing transition. However, the discrete jump is to a higher-energy one-pulse per round trip configuration. Thus instead of the pulse bifurcating to multi-pulsing solutions, the desired high-energy pulse is cleanly achieved. For this example, the transmission function was taken to be

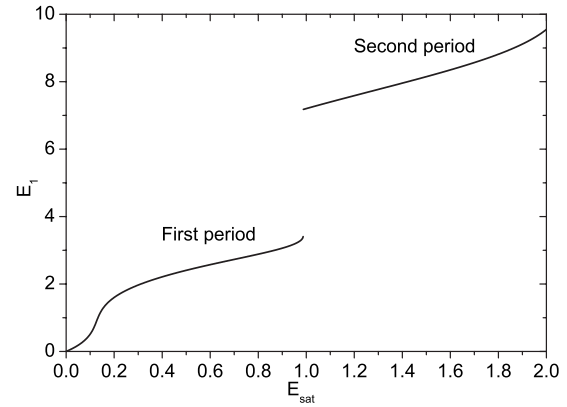


Fig. 15. Iteration map dynamics for the periodic nonlinear loss and saturating gain behavior of Fig. 14. Shown is the total cavity energy in the one-pulse solution. Note the jump to the high-energy branch.

$$T(E) = 0.02E + 0.1 + 0.2[1 + \cos((2 - \alpha_0 E)E - 0.8\pi)], \quad (5)$$

where $\alpha_0 = 0.08$. Note that the high-energy one-pulse solution has on average approximately three times the energy of the low-energy solution. Thus the laser cavity performance can be significantly enhanced with a passive means by proper engineering of the nonlinear loss curves.

A slight change in the transmission curve alters the ideal energy enhancement illustrated in Figs. 14 and 15. Simply changing the parameter α_0 to zero yields the transition behavior shown in Figs. 16 and 17. In this case, a jump from the low-energy one-pulse solution to the high-energy one-pulse solution occurs with a chaotic then periodic behavior. This is the reverse of the standard periodic to chaotic transmission. However, Fig. 16 exactly shows how this occurs in practice. In this case, as the one-pulse gain line jumps from the first period of the nonlinear loss to the second period, it begins by intersecting the chaotic dynamics region. As the gain is increased it then goes through a periodic region followed by the steady-state re-

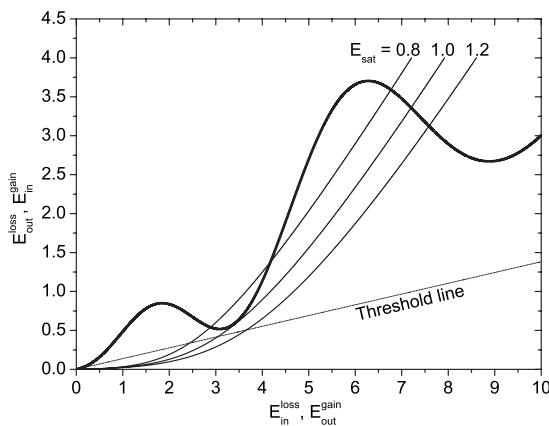


Fig. 14. Periodic nonlinear loss and saturating gain curves for one-pulse, two-pulse, and three-pulse per round trip configurations. The intersection of the gain and loss curves represents the mode-locked solution states of interest. As the cavity energy is increased, the gain curves shift to the right. The low-energy one-pulse solution ceases to exist beyond the threshold point forcing the solution to jump to a high-energy one-pulse solution.

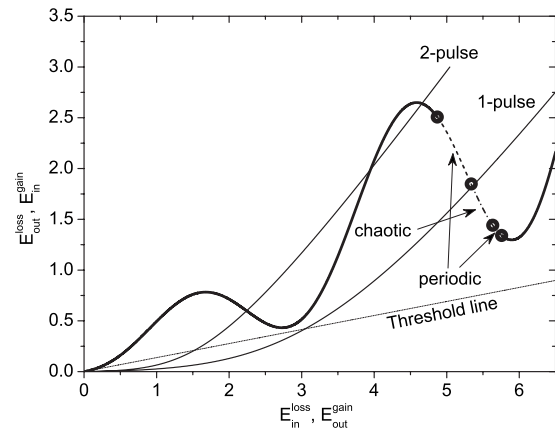


Fig. 16. Periodic nonlinear loss and saturating gain curves for one-pulse, two-pulse, and three-pulse per round trip configurations. The intersection of the gain and loss curves represents the mode-locked solution states of interest. As the cavity energy is increased, the gain curves shift to the right. The low-energy one-pulse solution ceases to exist beyond the threshold point forcing the solution to jump to a high-energy one-pulse solution. The solution jumps to a chaotic state.

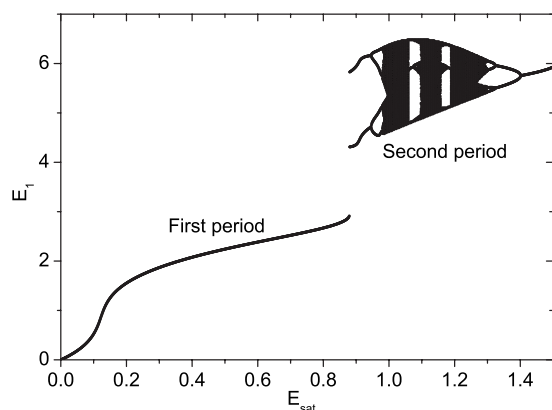


Fig. 17. Iteration map dynamics for the periodic nonlinear loss and saturating gain behavior of Fig. 16. Shown is the total cavity energy in the one-pulse solution. Note the chaotic, then periodic, jump to the high-energy branch.

gion. The desired steady-state mode-locking achieved in this case is essentially the same for Figs. 15 and 17. The routes to getting to the high-energy one-pulse solution, however, are quite different. Such simple geometrical modeling of the system conveys the practical power of the analysis and illustrates its impact on laser cavity design.

5. CONCLUSIONS

The multi-pulsing phenomenon is a ubiquitous instability of mode-locked laser cavities. Despite this well-known phenomenon, theoretical models capturing the transition dynamics and its associated bifurcations have been limited. The early work of Namiki *et al.* [3] was the first energy quantization approach used in computing the transition dynamics. This model presented a continuous picture of the multi-pulsing dynamics. More recent theoretical [4] and experimental [5,6] findings suggested the transition dynamics that displayed a behavior not considered by the original energy model formulation [3]. In this work, we have constructed a simple geometrical approach to quantifying the multi-pulse transition behavior. Only two equations are involved: the saturating gain [Eq. (1)] and the nonlinear losses described by a transmission function [Eq. (2)]. By iterating alternatively on these two effects, a complete multi-pulse transition picture can be constructed. The theory shows that the transition between N and $N+1$ pulses can be preceded by periodic and chaotic behavior as observed in recent experiments [5,6] and as suggested in theory [4].

The multi-pulsing instability ultimately is detrimental or undesirable for many applications where high-energy pulses are desired. Indeed, instead of achieving high-energy pulses as a consequence of increasing pump power, a multi-pulsing configuration is achieved with many pulses all of low energy. However, with the simple model presented here, it is easy to see that the laser cavity dynamics can be engineered simply by modifying the nonlinear loss curve. Of course, modification of the loss curve is trivial to do in theory, but may be difficult to achieve in practice. Regardless, the potential for an enhanced performance suggests that experimental modification of the nonlinear losses merits serious consideration and effort.

Specifically, we have demonstrated one potential periodic loss curve which suggests that instead of the cavity going through the multi-pulsing instability, it alternatively jumps to a high-energy solution branch, which is highly desired in practice. Indeed, a threefold increase in energy is demonstrated on average from a single jump in solution states. This essentially circumvents the limitations on pulse energy imposed by the multi-pulsing instability. In future work, we hope to use quantitative cavity models [21] to pursue a more careful study of the nonlinear loss curves generated from physically realistic cavity parameters.

ACKNOWLEDGMENTS

J. N. Kutz is especially thankful for discussions with Bjorn Sandstede, Brandon Bale, Frank Wise, William Renninger, Andy Chong, and Khan Kieu. J. N. Kutz acknowledges support from the National Science Foundation (NSF) (DMS-0604700) and the U.S. Air Force Office of Scientific Research (AFOSR) (FA9550-09-0174).

REFERENCES

1. H. A. Haus, "Mode-locking of lasers," *IEEE J. Sel. Top. Quantum Electron.* **6**, 1173–1185 (2000).
2. J. N. Kutz, "Mode-locked soliton lasers," *SIAM Rev.* **48**, 629–678 (2006).
3. S. Namiki, E. P. Ippen, H. A. Haus, and C. X. Yu, "Energy rate equations for mode-locked lasers," *J. Opt. Soc. Am B* **14**, 2099–2111 (1997).
4. J. N. Kutz and B. Sandstede, "Theory of passive harmonic mode-locking using waveguide arrays," *Opt. Express* **16**, 636–650 (2008).
5. B. G. Bale, K. Kieu, J. N. Kutz, and F. Wise, "Transition dynamics for multi-pulsing in mode-locked lasers," *Opt. Express* **17**, 23137–23146 (2009).
6. J. M. Soto-Crespo, M. Grapinet, P. Grelu, and N. Akhmediev, "Bifurcations and multiple-period soliton pulsations in a passively mode-locked fiber laser," *Phys. Rev. E* **70**, 066612 (2004).
7. Q. Xing, L. Chai, W. Zhang, and C. Wang, "Regular, period-doubling, quasi-periodic, and chaotic behavior in a self-mode-locked Ti:sapphire laser," *Opt. Commun.* **162**, 71–74 (1999).
8. B. Collings, K. Berman, and W. H. Knox, "Stable multigigahertz pulse train formation in a short cavity passively harmonic modelocked Er/Yb fiber laser," *Opt. Lett.* **23**, 123–125 (1998).
9. M. E. Fermann and J. D. Minelly, "Cladding-pumped passive harmonically mode-locked fiber laser," *Opt. Lett.* **21**, 970–972 (1996).
10. A. B. Grudinin, D. J. Richardson, and D. N. Payne, "Energy quantization in figure eight fibre laser," *Electron. Lett.* **28**, 67–68 (1992).
11. M. J. Guy, D. U. Noske, A. Boskovic, and J. R. Taylor, "Femtosecond soliton generation in a praseodymium fluoride fiber laser," *Opt. Lett.* **19**, 828–830 (1994).
12. M. Horowitz, C. R. Menyuk, T. F. Carruthers, and I. N. Duling III, "Theoretical and experimental study of harmonically modelocked fiber lasers for optical communication systems," *J. Lightwave Technol.* **18**, 1565–1574 (2000).
13. R. P. Davey, N. Langford, and A. I. Ferguson, "Interacting solutions in erbium fibre laser," *Electron. Lett.* **27**, 1257–1259 (1991).
14. M. J. Lederer, B. Luther-Davis, H. H. Tan, C. Jagadish, N. N. Akhmediev, and J. M. Soto-Crespo, "Multipulse operation of a Ti:Sapphire laser mode locked by an ion-implanted semiconductor saturable-absorber mirror," *J. Opt. Soc. Am. B* **16**, 895–904 (1999).

15. M. Lai, J. Nicholson, and W. Rudolph, "Multiple pulse operation of a femtosecond Ti:sapphire laser," *Opt. Commun.* **142**, 45–49 (1997).
16. C. Wang, W. Zhang, K. F. Lee, and K. M. Yoo, "Pulse splitting in a self-mode-locking Ti:sapphire laser," *Opt. Commun.* **137**, 89–92 (1997).
17. H. Kitano and S. Kinoshita, "Stable multipulse generation from a self-mode-locked Ti:sapphire laser," *Opt. Commun.* **157**, 128–134 (1998).
18. N. Akhmediev and A. Ankiewicz, *Dissipative Solitons*, Lecture Notes in Physics (Springer-Verlag, 2005).
19. R. Devaney, *An Introduction to Chaotic Dynamical Systems*, 2nd ed. (Addison-Wesley, 1989).
20. P. G. Drazin, *Nonlinear Systems* (Cambridge University Press, 1992).
21. E. Ding and J. N. Kutz, "Operating regimes, split-step modeling, and the Haus master mode-locking model," *J. Opt. Soc. Am. B* **26**, 2290–2300 (2009).